

Quantum noise spectra for periodically driven cavity optomechanics

E. B. Aranas* and M. Javed Akram

Department of Physics and Astronomy, University College London, Gower Street, London WC1E 6BT, United Kingdom

Daniel Malz

Cavendish Laboratory, University of Cambridge, Cambridge CB3 0HE, United Kingdom

T. S. Monteiro

Department of Physics and Astronomy, UCL, Gower Street, London WC1E 6BT, United Kingdom

(Received 31 October 2017; published 26 December 2017)

A growing number of experimental setups in cavity optomechanics exploit periodically driven fields. However, such setups are not amenable to analysis by using simple, yet powerful, closed-form expressions of linearized optomechanics, which have provided so much of our present understanding of experimental optomechanics. In the present paper, we formulate a method to calculate quantum noise spectra in modulated optomechanical systems, which we analyze, compare, and discuss with two other recently proposed solutions: we term these (i) frequency-shifted operators, (ii) Floquet [*Phys. Rev. A* **94**, 023803 (2016)], and (iii) iterative analysis [*New J. Phys.* **18**, 113021 (2016)]. We prove that (i) and (ii) yield equivalent noise spectra and find that (iii) is an analytical approximation to (i) for weak modulations. We calculate the noise spectra of a doubly modulated system describing experiments of levitated particles in hybrid electro-optical traps. We show excellent agreement with Langevin stochastic simulations in the thermal regime and predict squeezing in the quantum regime. Finally, we reveal how otherwise-inaccessible spectral components of a modulated system can be measured in heterodyne detection through an appropriate choice of modulation frequencies.

DOI: [10.1103/PhysRevA.96.063836](https://doi.org/10.1103/PhysRevA.96.063836)

I. INTRODUCTION

The last ten years have witnessed an impressive raft of experimental breakthroughs in the field of cavity quantum optomechanics [1]. Despite the enormous diversity of experimental setups (including membranes, microtoroids, photonic crystal microcavities and levitated nanoparticles among others), most experiments are amenable to analysis by means of the linearized theory of optomechanics. Through its well-established analysis in frequency space [1,2] one may obtain the *quantum noise spectra*, in other words, the spectra of fluctuations (whether quantum or classical) of optical and mechanical modes subjected to thermal and optical noises from the environment. This enabled valuable insights on the physics underlying optomechanical cooling [3–5], strong-coupling regimes [6], optical and mechanical squeezing [7–10], quantum backaction [11], as well as an understanding of the standard quantum limit (SQL) of optomechanical displacement sensing [1,2]. Hence, the analysis of quantum noise spectra from linearized optomechanical theory has become a ubiquitous tool of optomechanics.

Recently, however, a number of experimental setups have involved periodically driven fields. Here we do not allude to classical feedback fields, but rather to scenarios where cavity driving fields or other trapping fields are harmonically modulated in order to, for instance, generate mechanical squeezing [8–10] or even to simply improve the trapping and cooling [12–14] of levitated optomechanical systems. In such cases, even in regimes where nonlinearities are entirely absent

from dynamics, one may no longer adapt the textbook closed-form mathematical expressions for quantum noise spectra.

An optomechanical system comprising a single optical cavity mode coupled to a mechanical oscillator is described by the well-known Hamiltonian [1,2]:

$$\hat{H} = -\Delta\hat{a}^\dagger\hat{a} + \omega_M\hat{b}^\dagger\hat{b} + g(\hat{a}^\dagger + \hat{a})(\hat{b}^\dagger + \hat{b}), \quad (1)$$

where \hat{a} (\hat{a}^\dagger) is the annihilation (creation) operator for the optical mode, and \hat{b} (\hat{b}^\dagger) is the annihilation (creation) operator for the mechanical mode. Δ is the detuning between the input laser and the cavity, ω_M is the natural frequency of the mechanical oscillator, and g is the light-enhanced coupling strength. Constant Δ , ω_M , and g correspond to standard optomechanics. Dissipation is characterized by a single optical damping rate κ , and an intrinsic mechanical damping rate Γ_M . In the present work we consider the effects of modulating parameters such as Δ , ω_M , and g (see Fig. 1):

$$\hat{H}(t) = -\Delta(t)\hat{a}^\dagger\hat{a} + \omega_M(t)\hat{b}^\dagger\hat{b} + g(t)(\hat{a}^\dagger + \hat{a})(\hat{b}^\dagger + \hat{b}). \quad (2)$$

Several previous theoretical studies of modulated optomechanics were motivated by the quest to overcome the standard quantum limit (SQL) by measuring a single quadrature of the mechanical oscillator [15]. To date, two different ways to do single-quadrature detection have been proposed: one considered modulations of the optomechanical coupling g to perform backaction evasion (BAE) measurements [15,16], while the other considered modulation of ω_M to perform detuned mechanical parametric amplification (DMPA) [17,18]. Closely related schemes to generate mechanical squeezing are also of much interest. Modulation of the cavity field at $2\omega_M$ results in amplification of one quadrature and to squeezing of the conjugate quadrature [19,20]. The above studies all

*erika.aranas.14@ucl.ac.uk

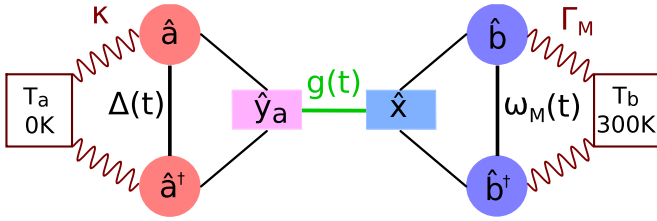


FIG. 1. Schematic of the modulated optomechanical Hamiltonian. \hat{a}, \hat{a}^\dagger and \hat{b}, \hat{b}^\dagger represent the optical and mechanical modes. The optical mode is driven by a strong coherent field, resulting in a linearized optomechanical coupling g that connects the optical amplitude quadrature $\hat{y}_a(t) = \frac{1}{\sqrt{2}}[\hat{a}(t) + \hat{a}^\dagger(t)]$ with the position quadrature $\hat{x}(t) = \frac{1}{\sqrt{2}}[\hat{b}(t) + \hat{b}^\dagger(t)]$. The system operators are coupled to their respective baths by κ for the zero-temperature optical bath, and by Γ_M for the mechanical bath at 300 K, leading to damping and dissipation. While for standard optomechanics g, ω_M, Δ are constant, we investigate here solutions for setups where they are harmonically modulated.

considered modulation either at or close to ω_M (resonant or near resonant); or modulation at a multiple (usually twice) of ω_M [19,21]. In addition, they considered modulation of *either* $g(t)$ [19,21] or of the spring constant [17,18].

In this paper we revisit periodically modulated optomechanics by analyzing a system [14] which involves not only simultaneous modulation of *both* g and ω_M , but also *far-off-resonant* modulation at frequencies $\ll \omega_M$. That study was motivated by the need to understand the distinctive optical sideband structure of the measured spectra from levitated nanoparticles in hybrid optical-electric traps [12,13]. In Ref. [14] an approximate, analytical solution was obtained for the quantum noise spectra of the optical field and mechanical displacement. The method produced closed-form expressions which successfully reproduced experimental spectral features, but only for the case of weak modulations.

Quantum noise spectra are obtained by transforming the corresponding quantum Langevin equations into frequency space; in the standard optomechanical case, these are frequently solved only for the individual mode of interest. However, a rather useful technique arises from so-called linear amplifier models [22,23] which cast the equations in a matrix form: $\mathbf{c}(\omega) = \mathbf{T}(\omega)\mathbf{c}_{\text{in}}(\omega)$, relating the input optical and mechanical noises to the field mode operator outputs by means of a transfer matrix \mathbf{T} . Here the vector $\mathbf{c}(\omega) = (\hat{a}(\omega)\hat{a}^\dagger(\omega)\hat{b}(\omega)\hat{b}^\dagger(\omega))^\top$ and the Gaussian input noise vector is $\mathbf{c}_{\text{in}}(\omega)$. We note that the $\hat{a}(\omega)$ solutions here denote the intracavity field (the actual detected cavity output field is then straightforwardly obtained by using the input-output relation $\hat{a}_{\text{out}}(\omega) = \hat{a}_{\text{in}}(\omega) - \sqrt{\kappa}\hat{a}(\omega)$ [24].

Such matrix methods have been used in previous studies of modulated optomechanics [19,21,25]. However, unlike the standard case, \mathbf{T} couples frequencies which differ by multiples of the modulation frequency. Its dimension is infinite so truncation becomes necessary. In this paper we identify two variants of the approach: in (i) the periodic Hamiltonian is expanded into a Fourier series, and a covariance matrix equation is obtained in terms of frequency-shifted system operators. (ii) In Ref. [21], a Floquet ansatz is used so

steady-state solutions are assumed to be periodic. This results in a Langevin equation for each Fourier component of the system operators which can be arranged into a matrix equation in Fourier space. Although in Ref. [19] a method equivalent to (i) was noted briefly, it has not previously been used to calculate quantum noise spectra.

We test the validity of the expressions of Ref. [14]—which we label method (iii)—in thermal and quantum regimes. The analytical expressions obtained by iterative solution in Ref. [14] are an approximate solution of method (i) for regimes where we may truncate the matrix \mathbf{T} to the lowest few orders. We also investigate the subtle, but interesting, differences between the two frequency space methods (i) and (ii). We prove that, although the matrix equations are apparently different, the methods, in fact, yield equivalent power spectra.

In Sec. III, we apply the formalism to the slowly modulated system in Ref. [14] where the frequencies $g(t)$ and $\omega_M(t)$ are modulated at a frequency $\omega_d \ll \omega_M$. A destructive interference process that leads to complete cancellation of one of the displacement sidebands offers a very stringent test of the calculations. We verify the results for the intracavity spectra in the thermal regime by numerical simulation of the slowly modulated, semiclassical Langevin equations by using a stochastic differential equation solver [26]. We also calculate the quantum homodyne spectra in the ponderomotive squeezing regimes (i.e., optical, not mechanical squeezing), even in the presence of strong modulations.

In Sec. IV we establish connections between the two methods (i) and (ii) to give a fuller picture of modulated optomechanical systems and their implications; in particular, by considering heterodyne detection of nonstationary spectral components which are usually inaccessible experimentally. Finally, we summarize and conclude in Sec. V.

II. THEORY: MATRIX METHODS FOR QUANTUM NOISE SPECTRA

For compactness and generality, we can extend Eq. (1) into an n -mode quadratic Hamiltonian $\hat{H}(t) = \frac{1}{2}\mathbf{c}^\top(t)\mathbf{H}(t)\mathbf{c}(t)$, where the Hamiltonian *matrix* $\mathbf{H}(t)$ contains the coupling frequencies between the modes and $\mathbf{c}(t) = [\hat{c}_1(t)\hat{c}_1^\dagger(t)\cdots\hat{c}_n(t)\hat{c}_n^\dagger(t)]^\top$ is a vector of $2n$ system operators. The resulting Heisenberg equation of motion is [27]

$$\dot{\mathbf{c}}(t) = -i\sigma\mathbf{H}(t)\mathbf{c}(t), \quad (3)$$

where we set $\hbar = 1$, and for bosonic ladder operators the canonical commutation relation (CCR) is

$$\sigma = [\mathbf{c}, \mathbf{c}^\dagger] = \bigoplus_{l=1}^n \begin{pmatrix} 1 & 0 \\ 0 & -1 \end{pmatrix}. \quad (4)$$

Each of the i th mode of $\mathbf{c}(t)$ is coupled to an infinite bath with rate γ_i which is described by a quantum Langevin equation:

$$\dot{\mathbf{c}}(t) = -i\sigma\mathbf{H}(t)\mathbf{c}(t) - \frac{\gamma}{2}\mathbf{c}(t) + \mathbf{c}_{\text{in}}(t), \quad (5)$$

where $\gamma = \text{diag}(\gamma_1, \gamma_1, \dots, \gamma_n, \gamma_n)$, and the *scaled* input noise operators $\mathbf{c}_{\text{in}}(t) \equiv (\sqrt{\gamma_1}\hat{c}_{\text{in},1}(t)\sqrt{\gamma_1}\hat{c}_{\text{in},1}^\dagger(t)\cdots\sqrt{\gamma_n}\hat{c}_{\text{in},n}(t)\sqrt{\gamma_n}\hat{c}_{\text{in},n}^\dagger(t))^\top$. They

are Gaussian noises which we assume to be δ correlated:

$$\begin{aligned} \langle \hat{c}_{in,i}(t)[\hat{c}_{in,i'}(t')]^\dagger \rangle &= (\bar{n}_i + 1)\delta_{ii'}\delta(t - t'), \\ \langle [\hat{c}_{in,i}(t)]^\dagger \hat{c}_{in,i'}(t') \rangle &= \bar{n}_i\delta_{ii'}\delta(t - t'), \end{aligned} \quad (6)$$

where we denote the $2i$ th element of $\mathbf{c}_{in}(t)$ by $\hat{c}_{in,i}$. The mode occupancy \bar{n}_i is set by the bath temperature. We further define a matrix of noise correlations in time:

$$\begin{aligned} \langle \mathbf{c}_{in}(t)[\mathbf{c}_{in}(t')]^\dagger \rangle &\equiv \mathbf{N}\delta(t - t') \\ &= \text{diag}(\gamma_1(\bar{n}_1 + 1) \gamma_1 \bar{n}_1 \cdots \\ &\quad \times \gamma_n(\bar{n}_n + 1) \gamma_n \bar{n}_n)\delta(t - t'). \end{aligned} \quad (7)$$

In the case of a time-independent Hamiltonian $\mathbf{H}(t) = \mathbf{H}$, Eq. (3) is diagonal in Fourier space:

$$\mathbf{c}(\omega) = \mathbf{T}(\omega)\mathbf{c}_{in}(\omega), \quad (8)$$

where the transfer matrix $\mathbf{T}(\omega) = (-i\omega\mathbf{I} + i\sigma\mathbf{H} + \frac{\gamma}{2})^{-1}$, \mathbf{I} is the identity matrix, and our convention for the Fourier transform is such that $[\mathbf{c}(\omega)]^\dagger = \int_{-\infty}^{+\infty} d\omega' e^{-i\omega t} [\mathbf{c}(t)]^\dagger$. Equation (8) underlines the essence of the linear amplifier model of standard optomechanics [23]: by working in frequency space we obtain the output noise from the input noise via simple matrix inversion.

The explicit time dependence of $\mathbf{H}(t)$ —slowly modulated or otherwise—prevents a straightforward application of the Fourier transform to obtain a matrix equation similar to Eq. (8). Nonetheless, one can apply Fourier techniques to Eq. (3) in two ways: (i) by Fourier expanding the Hamiltonian matrix, or (ii) by expanding both the Hamiltonian matrix and the system

operators [21]. One can then obtain a linear system either of frequency-shifted operators or of the Fourier components of the operators. In the following text we show the equivalence of methods (i) and (ii) by deriving the power spectrum under two assumptions: (1) input noise is Gaussian and stationary, and (2) no explicit time dependence is introduced in the signal during detection.

A. Method (i): Matrix equation of shifted operators

First we express the periodic Hamiltonian matrix as a Fourier series: $\mathbf{H}(t) = \sum_{k \in \mathbb{Z}} \mathbf{H}_k e^{ik\omega_d t}$. Equation (3) becomes

$$\dot{\mathbf{c}}(t) = \left(-i\sigma \sum_k \mathbf{H}_k e^{ik\omega_d t} - \frac{\gamma}{2} \right) \mathbf{c}(t) + \mathbf{c}_{in}(t), \quad (9)$$

which in frequency space becomes

$$\left[-i\omega\mathbf{I} + \frac{\gamma}{2} \right] \mathbf{c}(\omega) = -i\sigma \sum_k \mathbf{H}_k \mathbf{c}(\omega + k\omega_d) + \mathbf{c}_{in}(\omega). \quad (10)$$

Because of the time dependence of $\mathbf{H}(t)$ the vector $\mathbf{c}(\omega)$ depends on $\mathbf{c}(\omega + k\omega_d)$, preventing us from expressing Eq. (10) as a matrix equation similar to Eq. (8). Instead, we consider the shifted equations:

$$\begin{aligned} \left[-i(\omega + s\omega_d)\mathbf{I} + \frac{\gamma}{2} \right] \mathbf{c}(\omega + s\omega_d) \\ = -i\sigma \sum_k \mathbf{H}_k \mathbf{c}(\omega + (k+s)\omega_d) + \mathbf{c}_{in}(\omega + s\omega_d), \end{aligned} \quad (11)$$

for each k, s . A matrix equation of the form $\mathbf{c} = \mathbf{T}\mathbf{c}_{in}$ can then be obtained for the modulated system:

$$\begin{pmatrix} \vdots \\ \mathbf{c}(\omega + 2\omega_d) \\ \mathbf{c}(\omega + \omega_d) \\ \mathbf{c}(\omega) \\ \mathbf{c}(\omega - \omega_d) \\ \mathbf{c}(\omega - 2\omega_d) \\ \vdots \end{pmatrix} = \begin{pmatrix} \ddots & & & & & & \\ & \mathbf{X}(\omega + 2\omega_d) & \mathbf{A}_{-1} & \mathbf{A}_{-2} & & & \\ & \mathbf{A}_1 & \mathbf{X}(\omega + \omega_d) & \mathbf{A}_{-1} & & & \\ \cdots & \mathbf{A}_2 & \mathbf{A}_1 & \mathbf{X}(\omega) & & & \\ & \mathbf{A}_3 & \mathbf{A}_2 & \mathbf{A}_1 & \mathbf{X}(\omega - \omega_d) & & \\ & \mathbf{A}_4 & \mathbf{A}_3 & \mathbf{A}_2 & \mathbf{A}_1 & \mathbf{X}(\omega - 2\omega_d) & \\ & & & & & & \ddots \end{pmatrix}^{-1} \begin{pmatrix} \vdots \\ \mathbf{c}_{in}(\omega + 2\omega_d) \\ \mathbf{c}_{in}(\omega + \omega_d) \\ \mathbf{c}_{in}(\omega) \\ \mathbf{c}_{in}(\omega - \omega_d) \\ \mathbf{c}_{in}(\omega - 2\omega_d) \\ \vdots \end{pmatrix}, \quad (12)$$

where the $2n \times 2n$ matrix elements are

$$\mathbf{A}_s = i\sigma\mathbf{H}_s \quad (13)$$

$$\mathbf{X}(\omega + s\omega_d) = -i(\omega + s\omega_d)\mathbf{I} + i\sigma\mathbf{H}_0 + \frac{\gamma}{2}. \quad (14)$$

We denote s th row, l th column element of the transfer matrix as $\mathbf{T}_{sl}(\omega)$, with the central block being $[\mathbf{T}^{-1}]_{00}(\omega) = \mathbf{X}(\omega)$.

Our departure point to solve the measured power spectrum analytically is

$$\mathbf{S}_{cc^\dagger}(\omega) \equiv \lim_{T \rightarrow \infty} \langle \mathbf{c}(\omega)[\mathbf{c}(\omega)]^\dagger \rangle, \quad (15)$$

where we have generalized for now to the case of operators, and frequency-space variables are understood to be gated Fourier transforms: $\mathbf{c}(\omega) = \frac{1}{\sqrt{T}} \int_0^T dt e^{i\omega t} \mathbf{c}(t)$. Equation (15) is a $2n \times 2n$ matrix of spectra. We note that Ref. [21] offers a different

way to calculate the measured spectrum, but we come back to this point later in Sec. III C.

From Eq. (12) we know $\mathbf{c}(\omega) = \sum_{l \in \mathbb{Z}} \mathbf{T}_{0l}(\omega)\mathbf{c}_{in}(\omega - l\omega_d)$. Substituting this in Eq. (15) we obtain

$$\begin{aligned} \mathbf{S}_{cc^\dagger}(\omega) &= \lim_{T \rightarrow \infty} \sum_{l, l'} \mathbf{T}_{0l}(\omega) \langle \mathbf{c}_{in}(\omega - l\omega_d)[\mathbf{c}_{in}(\omega - l'\omega_d)]^\dagger \rangle \\ &\quad \times [\mathbf{T}_{0l'}(\omega)]^\dagger. \end{aligned} \quad (16)$$

It follows from Eq. (7) (proof in Appendix A) that

$$\lim_{T \rightarrow \infty} \langle \mathbf{c}_{in}(\omega - l\omega_d)[\mathbf{c}_{in}(\omega - l'\omega_d)]^\dagger \rangle = \mathbf{N}\delta_{ll'}. \quad (17)$$

Therefore,

$$\mathbf{S}_{cc^\dagger}(\omega) = \sum_{l \in \mathbb{Z}} \mathbf{T}_{0l}(\omega)\mathbf{N}[\mathbf{T}_{0l}(\omega)]^\dagger. \quad (18)$$

where the $Y_{\text{in}}(\omega)$ represent cavity-filtered incident shot noise (see Appendix B 2) and $\hat{x}(\omega)$ is the displacement of the mechanical oscillator.

We see that the only apparent significant change is to the mechanical displacement operators which are frequency shifted by the modulation. Hence it might be tempting to substitute standard optomechanics noise expressions for $\hat{x}(\omega)$ by simply shifting $\omega \rightarrow \omega \pm \omega_d$ and to directly solve the equation.

However, the most physically interesting effects [14] arise from cross correlations $\langle \hat{x}(\omega + \omega_d)\hat{x}(\omega - \omega_d) \rangle$ between the $\omega \pm \omega_d$ components, generated by the second ($2\omega_d$) modulation of $\omega_M(t)$.

An iterative analytical solution was developed for the operator $\hat{x}(\omega + \omega_d) - \hat{x}(\omega - \omega_d)$ (see Appendix B 2) which successfully reproduced experimental features, but remained accurate only for weak g and ω_2 . It is straightforward to see by inspection that the expressions used for the iterative solution are the central rows of Eq. (12) for $c(\omega)$: in other words, the iterative method is simply an approximation to the shifted operator method.

III. RESULTS: SIMULATION OF SPLIT-SIDEBAND SPECTRA

In this section we test and verify the expressions for the methods (i)–(iii)—both the iterative and the full matrix solution—against each other and against a numerical solution of the stochastic Langevin equations. Methods (i) and (ii) yield indistinguishable results. Both solutions show the same convergence properties in that they need to be truncated at a higher order as the modulations become stronger. To ensure invertibility and convergence, we truncate the matrix in Eq. (12) at an arbitrarily high odd dimension (17×17 block matrices).

For the numerics we explicitly solved a set of stochastic Langevin equations corresponding to the semiclassical dynamics of the system where we replace each operator in Eq. (B1) with its (in general complex) expectation value and its adjoint with the corresponding complex conjugates. The stochastic noises c_{in} have a Gaussian distribution with an average variance equal to the step size in the temporal propagation, such that $\langle c_{\text{in},i}(t)c_{\text{in},i'}^*(t') \rangle = \langle c_{\text{in},i}^*(t)c_{\text{in},i'}(t') \rangle = 2\pi(\bar{n} + 1/2)\delta_{i,i'}\delta(t - t')$.

A. Split-sideband spectra in strong-modulation regime

Figure 2 compares methods (i) and (ii) with method (iii) as well as with the numerical simulation of the intracavity spectrum of the doubly modulated system exhibiting the characteristic split-sideband separated by $2\omega_d$ about ω_M . To compare with previous studies [14], each spectrum is parametrized by both g and ω_2 . As was previously observed [14], the ratio of the split-sidebands change as the parameter ω_2/ω_d increases. Up to $\omega_2/\omega_d = 0.9$, all the three spectra exhibit progressively suppressed $\omega_M + \omega_d$ peak, and all show good agreement. From this point onward, however, the iterative solution fails to change the split-sideband ratio, while the full

solution matches very well with the numerics, even going past the complete suppression point at $\omega_2/\omega_d \approx \sqrt{2}$. We can also see this behavior in Fig. 2(b) where we plot the ratio of the split-sidebands as g and ω_2 increases. We also verify in Fig. 2(c) that the split-sideband ratio persists regardless of the cooperativity and is only determined by ω_2/ω_d . Depending on κ/ω_M , the split-sideband ratio may fluctuate before reaching a constant value. The higher the ω_2/ω_d the lower cooperativity is required to reach a constant ratio, so at the suppression point $r \approx 0$ for all C. We ensure that split sidebands are well resolved by choosing $\Gamma_{\text{opt}} \ll 2\omega_d$.

A new result of the comparison with the full Fourier methods (i) and (ii) is to provide a more accurate value of the point at which the second sideband is fully suppressed: here we observe the suppression point at $\omega_2/\omega_d \approx \sqrt{2}$. An earlier analysis of the based on the approximate method (iii) gives $\omega_2/\omega_d \sim 2$ [14]; however, that analysis of the low-order iterative solution neglected the modification to the susceptibilities due to higher-order backactions. The second sideband remains very weak across the entire $\omega_2/\omega_d \sim 1$ to 2 range, so the underlying physical explanation remains valid. Curiously, an even simpler model, using a Bessel expansion of the modulations in the interaction Hamiltonian [29], also predicts the more accurate $\omega_2/\omega_d \approx \sqrt{2}$ result.

B. Optical squeezing in homodyne spectra

Measured spectra detect the cavity output spectrum $\hat{a}_{\text{out}}(\omega) = \hat{a}_{\text{in}} - \sqrt{\kappa}\hat{a}(\omega)$, presenting additional interesting effects arising from correlations between the incoming noise and the intracavity field due to quantum backaction. In particular such correlations give rise to ponderomotive squeezing and power spectrum values below the shot-noise floor near $\omega \approx \omega_M$.

The measured homodyne spectrum detects a single optical quadrature:

$$i_{\text{hom}}(t) = e^{i\phi}\hat{a}_{\text{out}}(t) + e^{-i\phi}\hat{a}_{\text{out}}^\dagger(t), \quad (27)$$

and hence the measured power spectrum $S_{\text{hom}}(\omega) = \langle |i_{\text{hom}}(\omega)|^2 \rangle$ has four components: $S_{\text{hom}}(\omega) = \langle \hat{a}_{\text{out}}(\omega) [\hat{a}_{\text{out}}(\omega)]^\dagger \rangle + \langle [\hat{a}_{\text{out}}(\omega)]^\dagger \hat{a}_{\text{out}}(\omega) \rangle + \langle \hat{a}_{\text{out}}(\omega)\hat{a}_{\text{out}}(\omega) \rangle e^{2i\phi} + \langle [\hat{a}_{\text{out}}(\omega)]^\dagger [\hat{a}_{\text{out}}(\omega)]^\dagger \rangle e^{-2i\phi}$, and ϕ is the local oscillator phase ($\phi = 0$ for amplitude, and $\phi = \pi/2$ for phase quadrature).

Another advantage of the linear amplifier matrix formalism is that it outputs the full covariance matrix, facilitating calculation of the homodyne spectra which are constructed from several separate components. Usually, a probe mode different from the control beam is used for detection. When probe coupling is weak and $\Delta_p = 0$ it does not alter system dynamics but otherwise the probe could significantly couple to the oscillator motion regardless of the quadrature being measured. The matrix methods are extendable to any number of modes so we can easily incorporate probe dynamics.

Figure 3 shows the color map of the quantum homodyne spectra for the standard case, as well as the modulated case for three different modulation strengths. Large regions of squeezing of up to ≈ 1 dB (20% below the noise floor) can

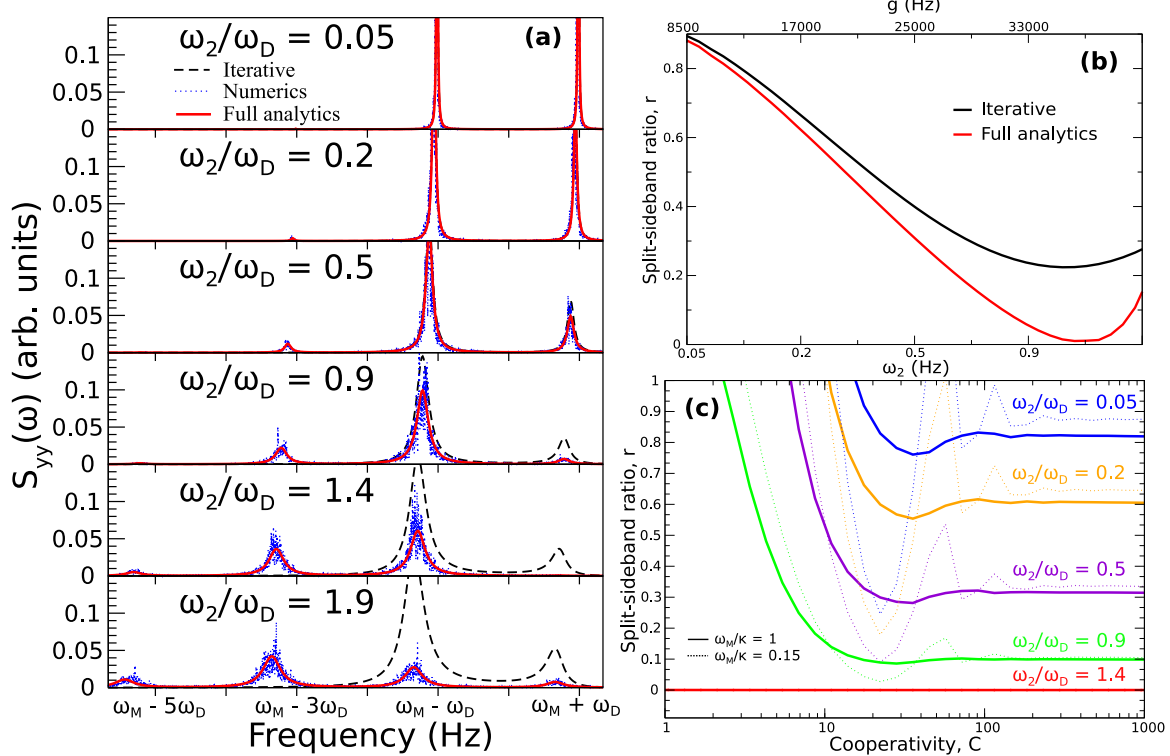


FIG. 2. (a) Comparison of the full analytical solution (red, solid) with the iterative solution (black, dashed) of the cavity spectrum $S_{yy}(\omega)$ for different values of ω_2/ω_d , with ω_d fixed. The stochastic numerics (blue, dotted) are obtained by solving the first-order coupled Langevin equations using XMDs2. There is good agreement among the three, where we see that one of the twin peaks is progressively suppressed until around $\omega_2/\omega_d = 0.9$, where from this point onward the iterative solution fails to show further suppression. The full analytical spectra, on the other hand, agree very well with numerics—even showing higher-order sidebands. The parameters are $\omega_d/\omega_M = 0.05$, $\Delta_2 = 0$, $\bar{n}_b = \frac{k}{\hbar\omega_M} 300$ K. (b) Sideband ratio vs g and ω_M for the same system as in panel (a). Note that the full analytical solution (red, lower) achieves the suppression point, after which the ratio bounces back to $R > 0$ as ω_2/ω_d is further increased. The g in panel (a) changes with each ω_2/ω_d and is given here in the alternative axis. (c) Split-sideband ratio vs cooperativity $C = \frac{4g^2}{\kappa\Gamma_M}$ for $\omega_2/\omega_d = 0.05, 0.2, 0.5, 0.9, 1.4$, and for both sideband resolved (solid, $\omega_M/\kappa = 1$) and otherwise (dotted, $\omega_M/\kappa = 0.15$). The parameters are $\omega_d/\omega_M = 0.05$, $\Delta_2 = 0$, $\bar{n}_b = \frac{k}{\hbar\omega_M} 300$ K. Split-sideband resolution is ensured by the condition $\Gamma_{\text{opt}} \ll 2\omega_d \Leftrightarrow \frac{C\Gamma_M}{2\omega_d} \ll 1$.

be observed for $0 < \phi < \pi/2$. The matrix method correctly replicates the squeezing profile of the standard case [7]. As expected for an on-resonance probe, the optical field shows no peaks at $\phi = 0$ while coupling most strongly with the mechanical oscillator at $\phi = \pi/2$. Optical squeezing at the mechanical frequency is impossible to see in standard optomechanics through homodyne detection, so sensing on-resonance will always be degraded by back-action noise, unless one performs a synodyne detection [30] or introduces modulations within the system [16,18].

Adding a slow modulation in $g(t)$ allows the measurement of the cross correlation $\langle \hat{x}(\omega + \omega_d)\hat{x}(\omega - \omega_d) \rangle$ that causes squeezing between the twin peaks. Introducing an additional periodicity in $\omega_M(t)$ at $2\omega_d$ further increases the contribution of the cross correlation. The result is a squeezed region that grows with ω_2/ω_d until it completely suppresses backaction noise (red) on resonance for $\omega_2/\omega_d \approx \sqrt{2}$. Such optical squeezing has been demonstrated for resonantly modulated optomechanical systems, but off-resonant modulated optomechanical systems could possibly offer a novel way of exploiting cross correlations for quantum sensing.

IV. DISCUSSION

Although we have shown that both methods (i) and (ii) give the same results for both intracavity- and homodyne-detected power spectra, we now investigate whether the equivalence holds for more general types of spectra. In particular, we discuss heterodyne detection of modulated optomechanical systems.

A. Connections between methods (i) and (ii)

In summary, for both methods a set of output field modes is obtained from a set of input noises by the action of a transfer matrix \mathbf{T} . However, in method (i) the output field operator $\mathbf{c}(\omega)$ originates from multiple, frequency-shifted input noise components $c_{\text{in}}(\omega + l\omega_d)$. In method (ii), in contrast, the dynamical operators were decomposed into a Fourier series $\mathbf{c}(t) = \sum_{l \in \mathbb{Z}} \mathbf{c}^{(l)}(t)e^{il\omega_d t}$. In this case these components $\mathbf{c}^{(l)}(\omega + l\omega_d)$ originate from the effect of the transfer matrix on a *single* input noise component $c_{\text{in}}(\omega)$.

To investigate these differences, we revisit once more the measured power spectra by rewriting Eq. (15) in terms of the

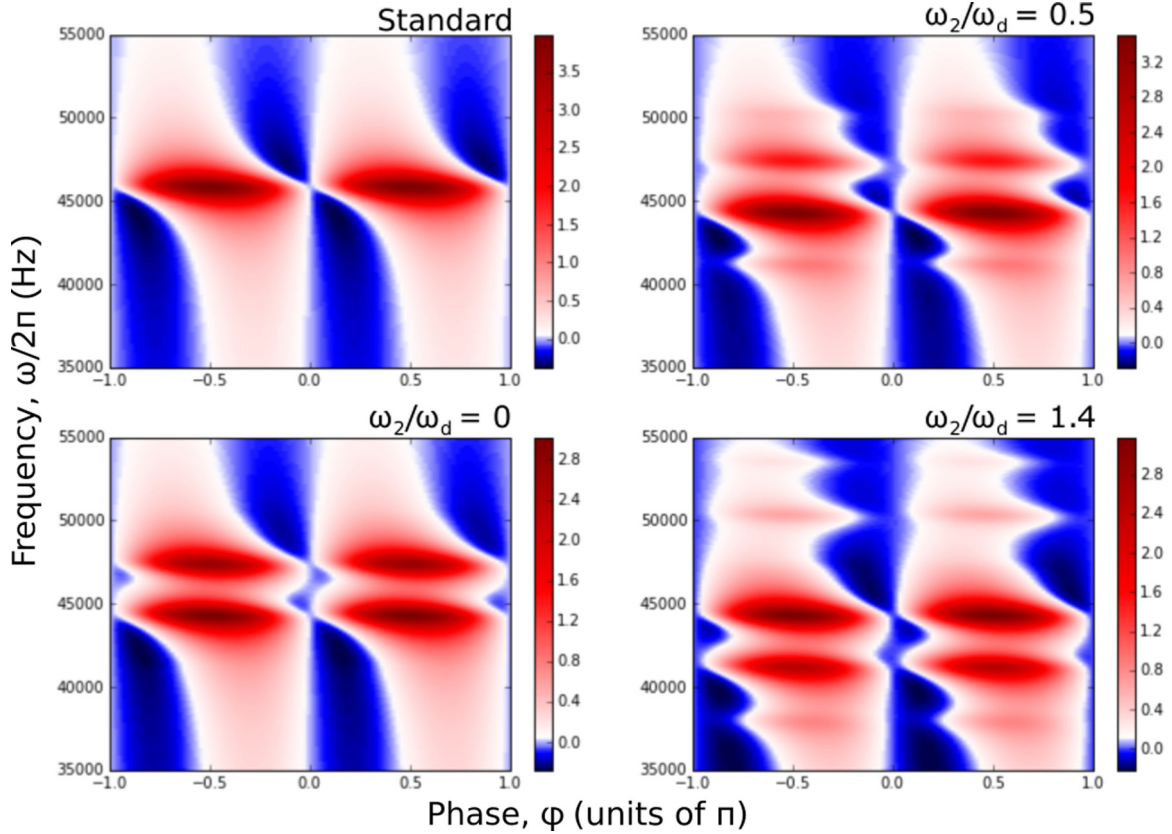


FIG. 3. Color map of the homodyne spectra $S_{\text{hom}}^{\phi}(\omega)$ versus the local oscillator (LO) angle ϕ for the standard case, as well as the slowly modulated cases with varying ω_2/ω_d . $g = 18.5$ kHz. We use two optical modes: the cooling mode at $\Delta = -\omega_M$ brings down the phonon occupation from 300 K to $\bar{n}_b < 1$ while the probe mode at $\Delta_p = 0$ is used for readout. Both are at $\bar{n}_a = 0$ and $\Gamma_M = 2.3 \times 10^{-5}$. The blue (red) region indicates noise below (above) the imprecision floor. We get a flat spectrum for the amplitude quadrature ($\phi = 0$), while a twin-peak around ω_M for the phase quadrature $\phi = \pi/2$. We show the color maps for the standard case, as well as for the slowly modulated case for three different ω_2/ω_d . Not only do we see familiar regions of squeezing characteristic to standard optomechanics, but also squeezing between the twin peaks. Maximum squeezing at ≈ 1 dB (20% below the noise floor) is achieved at $\phi = \pi/4$. At the suppression point $\omega_2/\omega_d \approx \sqrt{2}$ regions of high backaction noise (red) are replaced by squeezing. The rest of the parameters are the same as in Fig. 2(a).

autocorrelation function [2]:

$$\begin{aligned} \lim_{T \rightarrow \infty} \langle \mathbf{c}(\omega) [\mathbf{c}(\omega)]^{\dagger} \rangle &\equiv \lim_{T \rightarrow \infty} \frac{1}{T} \int_0^T dt \int_0^T d\tau e^{i\omega\tau} \\ &\quad \times \langle \mathbf{c}(t + \tau) [\mathbf{c}(t)]^{\dagger} \rangle \\ &= \lim_{T \rightarrow \infty} \frac{1}{T} \int_{-T/2}^{T/2} dt S(\omega, t), \end{aligned} \quad (28)$$

where $S(\omega, t)$ is defined as the Fourier transform of the autocorrelation function. For an ordinary (unmodulated) optomechanical system, the stationarity (i.e., time-translation invariance) of the stochastic process leads to the Wiener-Khinchin theorem: $\lim_{T \rightarrow \infty} \langle \mathbf{c}(\omega) [\mathbf{c}(\omega)]^{\dagger} \rangle = S(\omega)$ (independent of t).

In method (ii), the periodic modulation of $\mathbf{c}(t)$ naturally implies the periodic modulation of $S(\omega, t)$:

$$S(\omega, t) = \sum_{l \in \mathbb{Z}} S^{(m)}(\omega) e^{im\omega_d t}, \quad (29)$$

and in Ref. [21] it was shown that the measured spectrum is the zeroth-order component $S^{(0)}(\omega)$.

Although the higher-order spectral terms $S^{(m)}(\omega)$ appear to be experimentally inaccessible, we show below that these $|m| > 0$ contributions may be measured by using heterodyne detection with a beat frequency $2\Omega = n\omega_d$ resonant with the modulation. Hence the question arises as to how they can be calculated. It has been shown that $S^{(m)}(\omega)$ can be computed from the Fourier components of the operator by using method (ii) [21]. In Appendix C we show that the higher spectral components are, in fact, straightforwardly related to cross correlations between the method (i) operators:

$$\lim_{T \rightarrow \infty} \langle \mathbf{c}(\omega) [\mathbf{c}(\omega + m\omega_d)]^{\dagger} \rangle = S^{(m)}(\omega), \quad (30)$$

and hence higher-order components of the spectrum are also obtainable from method (i).

B. Measuring nonstationary spectrum components with heterodyne detection

Heterodyne detection measures a rotating quadrature:

$$i_{\text{het}}(t) = e^{i\phi + \Omega t} \hat{a}_{\text{out}}(t) + e^{-i(\phi + \Omega t)} a_{\text{out}}^{\dagger}(t), \quad (31)$$

and we take $\phi = 0$ as the power spectrum is in general insensitive to ϕ . Hence, in frequency space, $i_{\text{het}}(\omega) = \hat{a}_{\text{out}}(\omega + \Omega) + [\hat{a}_{\text{out}}(\omega - \Omega)]^\dagger$.

In getting the power spectrum $S_{\text{het}}(\omega) = \lim_{T \rightarrow \infty} \langle |i_{\text{het}}(\omega)|^2 \rangle$, intuition suggests that only the terms correlated at the same frequency will survive while the cross correlations will vanish. Another way to look at this is through the time domain, where the heterodyne signal in time will give rise to a time-dependent autocorrelator, and the cross terms carrying $\pm e^{2i\Omega t}$ will get averaged out in the Fourier transform [21]. Both viewpoints regarding the cancellation of cross correlations rely on the crucial fact that the noise is δ correlated. However, upon closer inspection, the cross correlations $\langle \hat{a}_{\text{out}}(\omega - \Omega) \hat{a}_{\text{out}}(\omega + \Omega) \rangle$ and $\langle [\hat{a}_{\text{out}}(\omega + \Omega)]^\dagger [\hat{a}_{\text{out}}(\omega - \Omega)]^\dagger \rangle$ can indeed be measured if the local oscillator frequency Ω is chosen appropriately. This is easy to show by using method (i):

$$\begin{aligned} & \lim_{T \rightarrow \infty} \langle \mathbf{c}(\omega + \Omega) [\mathbf{c}(\omega - \Omega)]^\dagger \rangle \\ &= \lim_{T \rightarrow \infty} \sum_{l, l' \in \mathbb{Z}} \mathbf{T}_{0l}(\omega + \Omega) \langle \mathbf{c}_{\text{in}}(\omega + l\omega_d + \Omega) \\ & \quad \times [\mathbf{c}_{\text{in}}(\omega + l'\omega_d - \Omega)]^\dagger [\mathbf{T}_{0l'}(\omega - \Omega)]^\dagger \\ & \quad \times \sum_{l \in \mathbb{Z}} \mathbf{T}_{0l}(\omega + \Omega) \mathbf{N}[T_{0, l+n}(\omega - \Omega)]^\dagger \rangle. \end{aligned} \quad (32)$$

The noise correlation in Eq. (7) forces $l' = l + n$, and also $n \equiv \frac{2\Omega}{\omega_d} \in \mathbb{Z}$. Such cross-correlations are useful in quantum sensing [20,30,31], and Eq. (32) illuminates the interesting fact that, by introducing an appropriate phase reference Ω —whether intrinsic to the system or externally—it becomes possible that a δ -correlated input noise (which vanishes if $\omega \neq \omega'$) can give rise to a nonzero correlation of output noises at different frequencies. In particular, we have shown how cross correlations (and hence, how rotating parts of the cavity output spectrum) can be recovered naturally in modulated systems by using heterodyne detection. The same idea has been applied on the level of rotating *mechanical* quadratures using the Fourier components of the periodic spectrum [21], which we know from Appendix C are equivalent to unequal-frequency cross correlations of shifted operators. Note also that quantum cross-correlations have been measured, but for a standard optomechanical system [31].

V. SUMMARY AND CONCLUSION

We present three approaches to solving quantum noise spectra of periodically modulated optomechanical systems: we call these (i) shifted operators, (ii) Floquet, and (iii) iterative methods. We prove that methods (i) and (ii) yield equivalent spectra, while method (iii) is an analytical approximation to method (i).

We compare the equivalent methods (i) and (ii) with Langevin stochastic simulations of the doubly modulated optomechanical Hamiltonian. The previously unexplored regime of slow but strong modulations in the optomechanical coupling and mechanical frequency provide a stringent test of the analytical methods. We demonstrate excellent agreement between methods (i) and (ii), confirming split-sideband suppression at $\omega_2/\omega_d \approx \sqrt{2}$. Method (iii), being effectively a low-order

truncation of the transfer matrix of method (i), also shows good agreement up to a certain modulation amplitude.

We also predict *resonant* squeezing in the quantum regime for the doubly modulated system as a result of enhanced cross-correlations in the shifted mechanical spectrum when $\omega_2/\omega_d \approx \sqrt{2}$. While squeezing at the mechanical frequency has been seen in other modulated schemes [16,30], we demonstrate possible new schemes for resonant squeezing in slowly modulated setups.

Finally, we obtain a fuller picture of the periodic character of the spectra of the Langevin solutions by establishing an explicit connection between unequal-frequency correlations of shifted operators and the Fourier components of the periodic spectrum. We also show how cross correlations (and hence, rotating components of the spectrum) are recovered by choosing the heterodyne local oscillator frequency to be resonant with the modulation of the optomechanical system.

ACKNOWLEDGMENTS

We are grateful for insightful discussions with Andreas Nunnenkamp. E.B.A. acknowledges fellowship support from the Schlumberger Faculty For the Future Program. M.J.A. is thankful for support through a Stocklin–Selmoni studentship. D.M. acknowledges DTA studentship support by the UK Engineering and Physical Sciences Research Council (EPSRC) under Grant No. EP/M506485/1.

APPENDIX A: FREQUENCY-SPACE NOISE CORRELATION IN TERMS OF KRONECKER DELTA

In this appendix we show that the noise correlation used to derive Eq. (18) follows from the δ correlation in time of Eq. (6):

$$\begin{aligned} & \lim_{T \rightarrow \infty} \langle \mathbf{c}_{\text{in}}(\omega + l\omega_d) [\mathbf{c}_{\text{in}}(\omega + l'\omega_d)]^\dagger \rangle \\ &= \lim_{T \rightarrow \infty} \left\langle \frac{1}{\sqrt{T}} \int_0^T dt e^{i(\omega + l\omega_d)t} \mathbf{c}_{\text{in}}(t) \right. \\ & \quad \times \left. \frac{1}{\sqrt{T}} \int_0^T dt' e^{-i(\omega + l'\omega_d)t'} [\mathbf{c}_{\text{in}}(t')]^\dagger \right\rangle \\ &= \lim_{T \rightarrow \infty} \frac{1}{T} \int_0^T dt e^{i(\omega + l\omega_d)t} \\ & \quad \times \int_0^T dt' e^{-i(\omega + l'\omega_d)t'} \langle \mathbf{c}_{\text{in}}(t) [\mathbf{c}_{\text{in}}(t')]^\dagger \rangle \\ &= \lim_{T \rightarrow \infty} \frac{1}{T} \int_0^T dt e^{i(\omega + l\omega_d)t} \int_0^T dt' e^{-i(\omega + l'\omega_d)t'} \mathbf{N}\delta(t - t') \\ &= \mathbf{N} \lim_{T \rightarrow \infty} \frac{1}{T} \int_0^T dt e^{i(l-l')\omega_d t} \\ &= \mathbf{N}\delta_{ll'}. \end{aligned} \quad (A1)$$

We can also generalize to the case of different frequencies that may arise from an external drive during detection. Assuming a frequency difference ω_{diff} , Eq. (A1) becomes

$$\lim_{T \rightarrow \infty} \langle \mathbf{c}_{\text{in}}(\omega + l\omega_d) [\mathbf{c}_{\text{in}}(\omega + \omega_{\text{diff}} + l'\omega_d)]^\dagger \rangle = \mathbf{N}\delta_{(l-l')\omega_d, \omega_{\text{diff}}}. \quad (A2)$$

The Kronecker δ forces ω_{diff} to be an integer multiple of ω_d . In the case of Eq. (32), we take $\omega_{\text{diff}} = 2\Omega$. For $\omega_{\text{diff}} = 0$, Eq. (A2) simplifies to Eq. (A1).

APPENDIX B: ANALYSIS OF SLOWLY MODULATED SYSTEM

In this appendix we apply the general formalism in Sec. II to analyze in detail the slowly modulated optomechanical

$$\begin{pmatrix} \dot{\hat{a}}(t) \\ \dot{\hat{a}}^\dagger(t) \\ \dot{\hat{b}}(t) \\ \dot{\hat{b}}^\dagger(t) \end{pmatrix} = \begin{pmatrix} i\Delta(t) - \frac{\kappa}{2} & 0 & ig(t) & ig(t) \\ 0 & -i\Delta(t) - \frac{\kappa}{2} & -ig(t) & -ig(t) \\ ig(t) & ig(t) & -i\omega_M(t) - \frac{\Gamma_M}{2} & 0 \\ -ig(t) & -ig(t) & 0 & i\omega_M(t) - \frac{\Gamma_M}{2} \end{pmatrix} \begin{pmatrix} \hat{a}(t) \\ \hat{a}^\dagger(t) \\ \hat{b}(t) \\ \hat{b}^\dagger(t) \end{pmatrix} + \begin{pmatrix} \sqrt{\kappa}\hat{a}_{\text{in}}(t) \\ \sqrt{\kappa}\hat{a}_{\text{in}}^\dagger(t) \\ \sqrt{\Gamma_M}\hat{b}_{\text{in}}(t) \\ \sqrt{\Gamma_M}\hat{b}_{\text{in}}^\dagger(t) \end{pmatrix}. \quad (\text{B1})$$

2. Iterative analytical method

We review the iterative method to obtain a quantum solution that is valid in the low order, as previously introduced in Ref. [14]. From Eq. (B1), the time-domain Langevin equations for the system operators are

$$\begin{aligned} \dot{\hat{a}}(t) &= \left[i\Delta(t) + \frac{\kappa}{2} \right] \hat{a}(t) + ig(t)[\hat{b}(t) + \hat{b}^\dagger(t)] + \sqrt{\kappa}\hat{a}_{\text{in}}(t), \\ \dot{\hat{b}}(t) &= -\left[i\omega_M(t) + \frac{\Gamma_M}{2} \right] \hat{b}(t) + ig(t)[\hat{a}(t) + \hat{a}^\dagger(t)] \\ &\quad + \sqrt{\Gamma_M}\hat{b}_{\text{in}}(t). \end{aligned} \quad (\text{B2})$$

Let us consider the specific case of a slowly modulated optomechanical system where

$$\begin{aligned} g(t) &= 2\bar{g} \sin \omega_d t, \\ \omega_M(t) &= \bar{\omega}_M + 2\omega_2 \cos 2\omega_d t, \\ \Delta(t) &= \bar{\Delta}. \end{aligned} \quad (\text{B3})$$

Defining $\hat{x}(t) = \frac{1}{\sqrt{2}}[\hat{b}(t) + \hat{b}^\dagger(t)]$ and $\hat{y}(t) = \frac{1}{\sqrt{2}}[\hat{a}(t) + \hat{a}^\dagger(t)]$, we obtain from Eq. (B2) the position and optical amplitude quadratures in frequency space, respectively:

$$\begin{aligned} \hat{x}(\omega) &= i\bar{g}\mu(\omega)[\hat{y}(\omega + \omega_d) - \hat{y}(\omega - \omega_d)] \\ &\quad + \sqrt{\Gamma_M}\hat{X}_{\text{th}}(\omega) + i\omega_2\mathcal{G}(\omega), \\ \hat{y}(\omega) &= i\bar{g}\eta(\omega)[\hat{x}(\omega + \omega_d) - \hat{x}(\omega - \omega_d)] + \sqrt{\kappa}\hat{Y}_{\text{in}}(\omega), \end{aligned} \quad (\text{B4})$$

where the optical and mechanical susceptibilities are

$$\begin{aligned} \chi_O(\omega) &= \left[-i(\omega + \bar{\Delta}) + \frac{\kappa}{2} \right]^{-1}, \\ \chi_M(\omega) &= \left[-i(\omega - \bar{\omega}_M) + \frac{\Gamma_M}{2} \right]^{-1}, \\ \mu(\omega) &= \chi_M(\omega) - \chi_M^*(-\omega), \\ \eta(\omega) &= \chi_O(\omega) - \chi_O^*(-\omega). \end{aligned} \quad (\text{B5})$$

system used to model levitated nanoparticles in a hybrid electro-optical trap.

1. Time-periodic Langevin equations

Let $\mathbf{c}(t) \equiv (\hat{a}(t) \hat{a}^\dagger(t) \hat{b}(t) \hat{b}^\dagger(t))^\top$ and denote the $2l$ th element of $\mathbf{c}(t)$ by \hat{c}_l so that $\hat{c}_1 \equiv \hat{a}$ and $\hat{c}_2 \equiv \hat{b}$. The optical and mechanical modes are coupled to their baths at κ and Γ_M , respectively, so $\gamma = \text{diag}(\kappa \kappa \Gamma_M \Gamma_M)$. After symmetrizing Eq. (1) and using the CCR equation (4), Eq. (3) for the optomechanical system is, explicitly,

The input noise is

$$\begin{aligned} \hat{X}_{\text{th}}(\omega) &= \chi_M(\omega)\hat{b}_{\text{in}}(\omega) + \chi_M^*(-\omega)\hat{b}_{\text{in}}^\dagger(\omega), \\ \hat{Y}_{\text{in}}(\omega) &= \chi_O(\omega)\hat{a}_{\text{in}}(\omega) + \chi_O^*(-\omega)\hat{a}_{\text{in}}^\dagger(\omega), \end{aligned} \quad (\text{B6})$$

and the correction due to ω_M excursion is $\mathcal{G}(\omega) \equiv \chi_M(\omega + 2\omega_d)\hat{b}(\omega + 2\omega_d) + \chi_M(\omega - \omega_d)\hat{b}(\omega - 2\omega_d) - \text{H.c.}$

To calculate the power spectral density (PSD) we need to express the system operators solely in terms of input noises. Note, however, from Eq. (B4) that the output vectors in ω not only depend on input noises at ω but also at system operators at $\omega \pm \omega_d$ and $\omega \pm 2\omega_d$. Hence we shift the quantum Langevin equations:

$$\begin{aligned} \hat{x}(\omega \pm n\omega_d) &= \pm i\bar{g}[\hat{y}(\omega \pm (n+1)\omega_d) - \hat{y}(\omega \pm (n-1)\omega_d)] \\ &\quad + \sqrt{\Gamma_M}\hat{X}_{\text{th}}(\omega \pm n\omega_d) + i\omega_2\mathcal{G}(\omega \pm n\omega_d), \\ \hat{y}(\omega \pm n\omega_d) &= \pm i\bar{g}[\hat{x}(\omega \pm (n+1)\omega_d) - \hat{x}(\omega \pm (n-1)\omega_d)] \\ &\quad + \sqrt{\kappa}\hat{Y}_{\text{in}}(\omega \pm n\omega_d), \end{aligned} \quad (\text{B7})$$

and iteratively substitute in Eq. (B4) the shifted vectors $\hat{x}(\omega \pm n\omega_d)$ and $\hat{y}(\omega \pm n\omega_d)$ for any $n \in \mathbb{Z}$ as they arise. Once we have $\hat{y}(\omega) = \sum_{l,n} \mathcal{A}_{c_l}(\omega + n\omega_d)\hat{c}_{\text{in},l}(\omega + n\omega_d) + \mathcal{A}_{c_l}^\dagger(\omega + n\omega_d)\hat{c}_{\text{in},l}^\dagger(\omega + n\omega_d)$, the power spectrum is simply $S_{yy}(\omega) = \sum_l |\mathcal{A}_{c_l}(\omega + n\omega_d)|^2 \bar{n}_l + |\mathcal{A}_{c_l}^\dagger(\omega + n\omega_d)|^2 (\bar{n}_l + 1)$.

As noise from higher orders is considered, the iterative method becomes increasingly accurate but equally cumbersome if done by hand. In the following we apply the method in Sec. (II A) to the slowly modulated optomechanical system with $n = 2$.

3. Matrix equation for slowly modulated system

Equation (12) is a general equation that computes the system operators from the input noises for any n -mode modulated optomechanical system. To get the equation for a slowly modulated system we set $\mathbf{c}(\omega + m\omega_d) \equiv (\hat{a}(\omega + m\omega_d) \hat{a}^\dagger(\omega + m\omega_d) \hat{b}(\omega + m\omega_d) \hat{b}^\dagger(\omega + m\omega_d))^\top$ and $\mathbf{c}_{\text{in}}(\omega) \equiv (\sqrt{\kappa}\hat{a}_{\text{in}}(\omega) \sqrt{\kappa}\hat{a}_{\text{in}}^\dagger(\omega) \sqrt{\Gamma_M}\hat{b}_{\text{in}}(\omega) \sqrt{\Gamma_M}\hat{b}_{\text{in}}^\dagger(\omega))^\top$. Moreover, the matrix elements are derived from the Hamiltonian Eq. (1) and

the parameters in Eq. (B3) by using Eq. (13) and Eq. (14):

$$X_n = \text{diag}(\chi_O(\omega + n\omega_d) \times \chi_O^*(-\omega - n\omega_d) \chi_M(\omega + n\omega_d) \chi_M^*(-\omega - n\omega_d)), \quad (\text{B8})$$

$$A_{\pm 1} = \pm \bar{g} \begin{pmatrix} & 1 & & 1 \\ & & -1 & -1 \\ 1 & & 1 & \\ -1 & -1 & & \end{pmatrix}, \quad (\text{B9})$$

$$A_{\pm 2} = i \begin{pmatrix} -\Delta_2 & 0 & & \\ 0 & \Delta_2 & & \\ & & \omega_2 & 0 \\ & & 0 & -\omega_2, \end{pmatrix}. \quad (\text{B10})$$

$A_{|m|>2} = 0$ because we do not consider here modulations greater than $2\omega_d$. We substitute (B8) to (B10) in the matrix equation (12) and calculate the power spectrum using Eq. (18).

APPENDIX C: COMPONENTS OF THE PERIODIC SPECTRUM IN TERMS OF SHIFTED OPERATORS

We show that the components of the periodic spectrum can also be calculated by using the shifted-operators approach where they have a new interpretation as cross correlations of operators shifted at different frequencies.

As mentioned Sec. III C, the assumption of the Floquet formalism is a periodic spectrum $S(\omega, t) = \sum_{m \in \mathbb{Z}} S^{(m)}(\omega) e^{im\omega_d t}$

with Fourier components [21]:

$$\begin{aligned} S^{(m)}(\omega) &= \sum_l \int_{-\infty}^{+\infty} \frac{d\omega'}{2\pi} \langle \mathbf{c}^{(l)}(\omega + l\omega_d) [\mathbf{c}^{(l-m)}(\omega')]^\dagger \rangle \\ &= \sum_l \int_{-\infty}^{+\infty} \frac{d\omega'}{2\pi} \mathbf{T}_{l0}(\omega + l\omega_d) \langle \mathbf{c}_{\text{in}}(\omega) [\mathbf{c}_{\text{in}}(\omega')]^\dagger \rangle \\ &\quad \times [\mathbf{T}_{l-m,0}(\omega' + l\omega_d)]^\dagger \\ &= \sum_l \mathbf{T}_{l0}(\omega + l\omega_d) \mathbf{N}[\mathbf{T}_{l-m,0}(\omega + l\omega_d)]^\dagger, \quad (\text{C1}) \end{aligned}$$

where we have used Eq. (21) and the noise correlation of Eq. (7) expressed in frequency space.

Consider the cross correlation of shifted operators from method (i):

$$\begin{aligned} &\lim_{T \rightarrow \infty} \langle \mathbf{c}(\omega) [\mathbf{c}(\omega + m\omega_d)]^\dagger \rangle \\ &= \sum_{l \in \mathbb{Z}} \mathbf{T}_{0l}(\omega) \langle \mathbf{c}_{\text{in}}(\omega - l\omega_d) [\mathbf{c}_{\text{in}}(\omega - l\omega_d)]^\dagger \rangle [\mathbf{T}_{-m,l}(\omega)]^\dagger \\ &= \sum_l \mathbf{T}_{0l}(\omega) \mathbf{N}[\mathbf{T}_{-m,l}(\omega)]^\dagger = S^{(m)}(\omega), \quad (\text{C2}) \end{aligned}$$

where in the last line we have invoked the translation property of \mathbf{T} . We then see that the Fourier components of the Fourier spectrum can be calculated using method (i).

-
- [1] M. Aspelmeyer, T. J. Kippenberg, and F. Marquardt, *Rev. Mod. Phys.* **86**, 1391 (2014).
 - [2] W. P. Bowen and G. J. Milburn, *Quantum Optomechanics* (CRC Press, Taylor & Francis Group, Boca Raton, Florida, 2016).
 - [3] J. D. Teufel, T. Donner, D. Li, J. H. Harlow, M. S. Allman, K. Cicak, A. J. Sirois, J. D. Whittaker, K. W. Lehnert, and R. W. Simmonds, *Nature (London)* **475**, 359 (2011).
 - [4] J. Chan, T. P. Mayer Alegre, A. H. Safavi-Naeini, J. T. Hill, A. Krause, S. Groblacher, M. Aspelmeyer, and O. Painter, *Nature (London)* **478**, 89 (2011).
 - [5] E. Verhagen, S. Deleglise, S. Weis, A. Schliesser, and T. J. Kippenberg, *Nature (London)* **482**, 63 (2012).
 - [6] J. M. Dobrindt, I. Wilson-Rae, and T. J. Kippenberg, *Phys. Rev. Lett.* **101**, 263602 (2008).
 - [7] T. P. Purdy, P. L. Yu, R. W. Peterson, N. S. Kampel, and C. A. Regal, *Phys. Rev. X* **3**, 031012 (2013).
 - [8] E. E. Wollman, C. U. Lei, A. J. Weinstein, J. Suh, A. Kronwald, F. Marquardt, A. A. Clerk, and K. C. Schwab, *Science* **349**, 952 (2015).
 - [9] J.-M. Pirkkalainen, E. Damskagg, M. Brandt, F. Massel, and M. A. Sillanpää, *Phys. Rev. Lett.* **115**, 243601 (2015).
 - [10] F. Lecocq, J. B. Clark, R. W. Simmonds, J. Aumentado, and J. D. Teufel, *Phys. Rev. X* **5**, 041037 (2015).
 - [11] V. Jain, J. Gieseler, C. Moritz, C. Dellago, R. Quidant, and L. Novotny, *Phys. Rev. Lett.* **116**, 243601 (2016).
 - [12] J. Millen, P. Z. G. Fonseca, T. Mavrogordatos, T. S. Monteiro, and P. F. Barker, *Phys. Rev. Lett.* **114**, 123602 (2015).
 - [13] P. Z. G. Fonseca, E. B. Aranas, J. Millen, T. S. Monteiro, and P. F. Barker, *Phys. Rev. Lett.* **117**, 173602 (2016).
 - [14] E. B. Aranas, P. Z. G. Fonseca, P. F. Barker, and T. S. Monteiro, *New J. Phys.* **18**, 113021 (2016).
 - [15] C. M. Caves, K. S. Thorne, R. W. P. Drever, V. D. Sandberg, and M. Zimmermann, *Rev. Mod. Phys.* **52**, 341 (1980).
 - [16] A. A. Clerk, F. Marquardt, and K. Jacobs, *New J. Phys.* **10**, 095010 (2008).
 - [17] A. Szorkovszky, A. A. Clerk, A. C. Doherty, and W. P. Bowen, *New J. Phys.* **16**, 043023 (2014).
 - [18] B. A. Levitan, A. Metelmann, and A. A. Clerk, *New J. Phys.* **18**, 093014 (2016).
 - [19] A. Mari and J. Eisert, *Phys. Rev. Lett.* **103**, 213603 (2009).
 - [20] A. Kronwald, F. Marquardt, and A. A. Clerk, *Phys. Rev. A* **88**, 063833 (2013).
 - [21] D. Malz and A. Nunnenkamp, *Phys. Rev. A* **94**, 023803 (2016).
 - [22] A. A. Clerk, M. H. Devoret, S. M. Girvin, F. Marquardt, and R. J. Schoelkopf, *Rev. Mod. Phys.* **82**, 1155 (2010).
 - [23] T. Botter, D. W. C. Brooks, N. Brahms, S. Schreppler, and D. M. Stamper-Kurn, *Phys. Rev. A* **85**, 013812 (2012).
 - [24] C. W. Gardiner and M. J. Collett, *Phys. Rev. A* **31**, 3761 (1985).
 - [25] G. A. Peterson, F. Lecocq, K. Cicak, R. W. Simmonds, J. Aumentado, and J. D. Teufel, *Phys. Rev. X* **7**, 031001 (2017).
 - [26] G. R. Dennis, J. J. Hope, and M. T. Johnsson, *Comput. Phys. Commun.* **184**, 201 (2013).
 - [27] A. Serafini, *Quantum Continuous Variables: Quantum Entanglement, Communication and Control* (CRC Press, Taylor & Francis Group, Boca Raton, Florida, 2017).

- [28] D. Malz and A. Nunnenkamp, *Phys. Rev. A* **94**, 053820 (2016).
- [29] E. B. Aranas, P. Z. G. Fonseca, P. F. Barker, and T. S. Monteiro, *J. Opt. (Bristol, U. K.)* **19**, 034003 (2017).
- [30] L. F. Buchmann, S. Schreppler, J. Kohler, N. Spethmann, and D. M. Stamper-Kurn, *Phys. Rev. Lett.* **117**, 030801 (2016).
- [31] T. P. Purdy, K. E. Grutter, K. Srinivasan, and J. M. Taylor, *Science* **356**, 1265 (2017).